Small Angle Neutron Scattering Study of Structural Aspects of Nonionic Surfactants (Tween 20 and Tween 80) in the Presence of Polyethylene Glycols and Triblock Polymers

Rakesh Kumar Mahajan,[1] Jyoti Chawla,[1] Kulwinder Kumar Vohra,[1] Vinod Kumar Aswal[2]

[1]*Department of Chemistry, Guru Nanak Dev University, Amritsar 143005, India*
[2]*Solid State Physics Division, Bhabha Atomic Research Centre, Mumbai 400085, India*

Received 7 September 2009; accepted 13 December 2009
DOI 10.1002/app.32134
Published online 29 April 2010 in Wiley InterScience (www.interscience.wiley.com).

ABSTRACT: Small angle neutron scattering (SANS) technique has been used to study the micellar behavior of nonionic surfactants, Tween 20 and Tween 80 with additives like polyethylene glycols (PEG with molecular mass 400, 6000, and 15,000) and triblock polymers (TBPs) of varying composition. Surfactant-additive interactions have been explained on the basis of parameters like aggregation number (N_{agg}), core radius (R_c), hard sphere radius (R_{hs}), volume fraction (ϕ) and axial ratio (b/a). The SANS analysis indicate the reduction in values of N_{agg} of Tween on addition of PEG additive. Shape of Tweens (3 wt %) micelles in the presence of PEG (10 wt %) is found to oblate ellipsoidal. Similarly, the shape of Tween (3 wt %) micelles is oblate ellipsoidal at low concentration of TBPs (1 wt %); however, they become spherical as the concentration of TBP increases to 10 wt %. The shape of micelles of pure TBPs also comes out to be spherical. Results reflects that at low concentration of TBP shape is controlled by surfactant (Tween 20 and Tween 80) while at high concentration of TBP shape of mixed micelle is controlled by TBP. © 2010 Wiley Periodicals, Inc. J Appl Polym Sci 117: 3038–3046, 2010

Key words: Tweens; polyethylene glycols; triblock polymer; SANS studies; aggregation

INTRODUCTION

Mixing two or more surfactants has been a common and yet beneficial practice in industries to formulate products with desired properties that are not achievable from the individual surfactants by themselves.[1] To optimize the applications of surfactant mixtures, research enthusiasm has never ceased in probing the properties of surfactant mixtures. Polymer and surfactants are very often used in combination in cosmetic, medicinal, and pharmaceutical preparations. These are also used in injecting fluid for the enhanced oil recovery process. The study of surfactant/polymer mixture is therefore also of potential importance in the applied surface-chemical field. Since different types of surfactants exist, various kinds of combinations are possible with different properties and application fields. Solution mixtures of some surfactant systems have been well studied while some are less explored.[2]

It is well known[3,4] that polyethylene nonionic surfactants interact attractively with both anionic and cationic surfactants such as sodium dodecyl sulfate (SDS) and dodecylammonium chloride, respectively, in adsorbed films and micelles. Interactions between nonionic surfactant and nonionic polymer are difficult to explain as the critical micelle concentration (CMC) is smaller than those of the ionic counterparts and the micelle interface is not as clear as for ionic surfactant micelles. Nonionic surfactants are often considered to be indifferent to nonionic polymers and are considered not to interact or very weakly interact with the polymers.[5] Hydrophilic nonionic polymers do not interact with polyoxyethylenated surfactant. If, however, the polymer contains hydrophobic segments in its molecule, nonionic surfactant can interact with such polymers due to hydrophobic interactions between surfactant and polymer hydrophobic segments. However, relatively few investigations related to these systems have been carried out.[6,7]

The ethoxylated sorbitan esters (Tweens) are a large class of nonionic surfactants. The groups that are attached to the sorbitan include oleate, palmitate,

Correspondence to: R. K. Mahajan (rakesh_chem@yahoo.com).

Contract grant sponsors: IUC-DAE (BARC).

stearate, and ethoxylated versions of each of these. The ethoxylated sorbitan esters are water soluble and used as industrial emulsifiers, antistatic agents, fiber lubricants, and solubilizers. These surfactants have been approved for human consumption. They do not produce ions in aqueous solution. As a consequence, they are compatible with other types and are excellent candidates to enter the complex mixtures, as found in many commercial products. They are much less sensitive to electrolytes, particularly divalent cations, than ionic surfactants. Glycols and triblock polymers (TBPs) are widely used in detergents, cosmetics, and many other industrial applications.[8–10] This is due to the fact that glycols have fascinating solvation behavior similar to that of water. Glycol oligomers not only change the medium properties but also effect the micelle formation even if they are used in substantial amount in aqueous solution. In the presence of water, glycol acts as water structure breaker, which leads to the formation of a new structure knitted with hydrogen bonding between the water and glycol molecules. Such a combined structured phase also provides a complete hydrophobic environment for amphiphilic molecules as of surfactants to assemble in a similar way as they do in pure water.[11–13] Polyethylene oxide–polypropylene oxide–polyethylene oxide (PEO–PPO–PEO) copolymers exist in different states of aggregation in aqueous solution depending on relative block sizes, concentration, and temperature. The self-association behavior of these copolymers in water has attracted great attention.[14,15] Single molecular species (unimers) dominate at low temperature and concentrations. At moderately high temperatures and concentrations, the PEO–PPO–PEO copolymers self-assemble to form micelles because of limited and temperature dependent solubility of PPO block. Their unique structure allows a novel approach in the design and application of surface-active agents. Most other nonionic surfactant classes limit the number of available hydrophobes and effect the changes in surfactant function only by altering the hydrophile. TBPs allow incremental alteration of both hydrophobe and hydrophile. In addition, alternating EO/PO structures can be introduced internally or at the end of the molecule.

It has been observed that the lower glycols significantly affect the process of micelle formation of both single and mixed surfactants because of their strong water structure breaking effects, whereas the higher ones prefer to adsorb at the micelle-solution interface or even form the polymer bound micellar aggregates.[16] The additive effect of glycols on micelle formation of nonionic surfactants is still not clear in comparison with that on the micelle formation of ionic surfactants, since former is considered to have very weak interactions in comparison with latter and a very few reports are available in literature. The aim of this article is to understand the Tween (nonionic surfactant)—glycol/TBP interactions by using small angle neutron scattering (SANS) measurements. The structural characteristics of aqueous solutions of Tween 20 and Tween 80 in the presence of polyethylene glycols (PEGs) and TBPs of poly(ethylene oxide)–poly(propylene oxide)–poly(ethylene oxide), PEO–PPO–PEO has been studied. It has been investigated that how glycols/TBPs affect the size, shape, and aggregation number of Tween micelles. A relative change in micellar parameters of Tween in the presence of glycols/TBPs with respect to its properties in pure water helps to quantitatively identify the preferential solvation of additives.

EXPERIMENTAL

Materials and methods

Tween 20 and Tween 80 were obtained from Lancaster Synthesis, UK. PEGs were products of CDH, Mumbai, India. TBP-TBP_5 was obtained from Hi-Media Laboratories, Mumbai, India. All other TBPs were received from Sigma and their characteristic features are listed in Table I. D_2O was obtained from heavy water plant of Bhabha Atomic Research Centre, Mumbai, India. All reagents were used as received and were of analytical grade.

SANS measurements

SANS measurements were performed using SANS instrument at DHRUVA reactor, Trombay.[17] DHRUVA is a high flux reactor (power = 100 MW). The neutron flux at Dhruva reactor at BARC is 1.4×10^{14} $N/cm^2/s$. In all the measurements, Tween concentration was kept constant (3 wt %) and the solutions were prepared in D_2O. The use of D_2O instead of water provides a better contrast between the micelle and the solvent during SANS experiments. A quartz cell of 0.5 cm path length was used to hold the samples. The sample temperature was maintained at 30°C. The Be-filter with double

TABLE I
Composition of Various TBPs (PEO–PPO–PEO)

Polymers	Molecular weight	Total no. of EO units (1/2 in equal no).	No. of PO units
TBP_1	1100	4	15.5
TBP_2	3400	36	31
TBP_3	2900	26	30
TBP_4	6500	74	56
TBP_5	8350	152	30
TBP_6	12600	194	69

monochromater is used to remove the wavelength contribution that comes from the second-order Bragg's diffraction. The beam size at the sample position was 1.5 cm × 1.0 cm. The scattered neutrons from the sample were detected using a 100-cm long and 3.8-cm diameter He^3 linear position sensitive detector. The distance between the sample and detector was 1.85 m for all runs. The accessible Q range of the instrument is 0.018–0.32 $Å^{-1}$. The data were corrected for background, empty-cell contribution and sample transmission, and normalized to absolute cross-section units.

RESULTS AND DISCUSSION

Details of data treatment

The scattering of neutron by a nucleus is characterized by a single parameter, b the nuclear scattering length. The neutron-nuclear interaction occurs over a distance very much smaller than the neutron wavelength (λ), so that the scattered wave is spherical. If the wave vectors of incident and scattered waves are K_i and K_f, respectively, a wave scattered by a nucleus at a point r in the sample will thus be a phase shifted with respect to scattering at the origin by a phase factor exp ($iQ.r$), where $Q = K_i - K_f$ is the wave vector transferred in the scattering process. The coherent differential scattering cross-section is the summation of the amplitude weighted phase shifts and can be expressed as follows:[18,19]

$$\frac{d\Sigma}{d\Omega}(Q) = \left\langle \left| \sum_j b_j \exp(iQ.r_j) \right|^2 \right\rangle \quad (1)$$

where b_j is the bound scattering length and r_j is the position vector of jth nucleus in sample, and bracket represents an average over all possible configurations. In the following, we shall write expression for $d\Sigma/d\Omega$ for a system consisting of particles dispersed in uniform medium for the use of SANS.[20,21]

The spatial resolution in the SANS experiments is much larger than the interatomic distance and thus it is not meaningful to talk of individual nuclei in the present discussion. Thus, we replace scattering length b_j in above equation by a locally averaged scattering length density ρ(r) and eq. (1) can be written as

$$\frac{d\Sigma}{d\Omega}(Q) = \left\langle \left| \int \rho(r) \exp(iQ.r) dr \right|^2 \right\rangle \quad (2)$$

where the integration is over the unit volume of the sample. ρ(r) is mathematically defined as

$$\rho(r) = \frac{1}{v(r)} \sum_i b_i \quad (3)$$

The summation in the above equation extends over all the nuclei in the volume element $v(r)$ around r. In general, the particle could be heterogeneous in its composition and it may not have uniform scattering length density. However, to simplify, it has been assumed that scattering length densities in the particle and the matrix are uniform. That is, sample is treated as a two-component system. Let ρ_p and ρ_m are the scattering length densities for the particle and the matrix or solvent, respectively. Then, eq. (2) can be written as

$$\frac{d\Sigma}{d\Omega}(Q) = \left\langle \left| \rho_p \int_{V_P} \exp(iQ.r) dr + \rho_m \int_{V_m} \exp(iQ.r) dr \right|^2 \right\rangle \quad (4)$$

The integration in the first term is over the volume V_P occupied by all particles and that in the second term is over the volume V_m occupied by the matrix. Above equation can be rewritten as

$$\frac{d\Sigma}{d\Omega}(Q) = \left\langle \left| (\rho_p - \rho_m) \int_{V_p} \exp(iQ.r) dr + \rho_m \left\{ \int_{Vm} \exp(iQ.r) dr + \int_{V_p} \exp(iQ.r) dr \right\} \right|^2 \right\rangle \quad (5)$$

The second term in above equation is the total scattering amplitude from a system in which the particle amplitude has been replaced by the solvent amplitude. This term is decided by the isothermal compressibility of the solvent and is negligible at low Q. Neglecting the second terms one obtains

$$\frac{d\Sigma}{d\Omega}(Q) = (\rho_p - \rho_m)^2 \left\langle \left| \int_{V_P} \exp(iQ.r) dr \right|^2 \right\rangle \quad (6)$$

The integration in above equation is over all the particles in sample. It may be noted that $V_p = nV$, where n is the number of particles per unit volume of the sample and V is the average volume of the single particle. The above integration contains spatial and orientational correlation between the particles and also effects arising due to the size distributions. To simplify the above equation, it can be rewritten as

$$\frac{d\Sigma}{d\Omega}(Q) = (\rho_p - \rho_m)^2 V^2 \left\langle \left| \sum_k F_k(Q) \exp(iQ.R_k \right|^2 \right\rangle \quad (7)$$

where R_k is the position vector of the center of kth particle and $F_k(Q)$ is the form factor associated with the particle. $F(Q)$ is defined as follows:

$$F(Q) = \frac{1}{V}\int_V \exp(iQ.r)dr \tag{8}$$

and is normalized so that $|F(0)|^2 = 1$.

Equation can also be written as

$$\frac{d\Sigma}{d\Omega}(Q) = (\rho_p - \rho_m)^2 V^2 \left[n\left\langle |F(Q)|^2 \right\rangle + \left\langle \sum_k \sum_{k'} F_k(Q) F_{k'}^*(Q) \exp(iQ.(R_k - R_{k'})) \right\rangle \right] \tag{9}$$

The summation in the second term extends over all the n particles in the sample. It is seen that the scattering cross-section from a collection of particles consists of two terms, the first of which depends on the intraparticle scattering and the second on interparticle scattering. The intraparticle scattering is the average of the square of the particle form factor and is denoted by $P(Q)$. This term depends on the shape and size of the particle and in principle can be calculated for any geometry. The interparticle interference term can be evaluated in a closed form only if certain assumptions are made about the correlation between the spacing of the particles and their sizes and orientations. The simplest assumption is that sample contains monodispersed spherical particles, for which above equation can be simplified to the form

$$\frac{d\Sigma}{d\Omega}(Q) = n(\rho_p - \rho_m)^2 V^2 P_{sp}(Q) S(Q) \tag{10}$$

where $P_{sp}(Q)$ is the intraparticle structure factor for a spherical particle. $S(Q)$ is the interparticle structure factor. $S(Q)$ is given by

$$S(Q) = 1 + \frac{1}{n}\left\langle \sum_k \sum_{k'} \exp[iQ.(R_k - R_{k'})] \right\rangle \tag{11}$$

Intraparticle structure factor $P(Q)$ depends on the shape and size of the particles. Dilute systems are ideally suited for studying the shapes and sizes of the particles. In these systems, the particles concentration is very low. As the interparticle distances are much larger than the particle size in the systems, the interparticle interference is negligible and $S(Q) \sim 1$. Thus, the scattering distribution depends on the functionality of the $P(Q)$. Equation (1) for dilute system may be written as

$$\frac{d\Sigma}{d\Omega}(Q) = n(\rho_p - \rho_m)^2 V^2 P(Q) \tag{12}$$

The expressions for $P(Q)$ for different structures of the particles are available.[22]

The expressions for some of the shapes (discussed in this study) are given below:

1. Spherical shape: For a sphere of radius R

$$P(Q) = \left[\frac{3(\sin QR - QR\cos QR}{(QR)^3} \right]^2 \tag{13}$$

2. Ellipsoidal shape: $P(Q)$ for an ellipsoidal particle is given by equation

$$P(Q) = \int [F(Q,\mu)]^2 d\mu \tag{14}$$

The form factor $F(Q,\mu)$ is given by eq. (3), i.e.,

$$F(Q,\mu)] = 3(\sin w - w\cos w)/w^3 \tag{15}$$

where $w = Q[a^2\mu^2 + b^2(1-\mu^2)]^{1/2}$. μ is the cosine of the angle between the directions of major axis and the wave vector transfer Q, and a, b are respectively the semiminor and semimajor axes of the ellipsoid of revolution. That is, $P(Q)$ depends on values of (a) and (b).

SANS behavior of Tweens (3 wt %) in the presence of glycols (10 wt %)

The SANS data for Tween 20 and Tween 80 in the presence of various polyethylene glycols at 30°C is shown in Figures 1 and 2. Solid lines in figures are the fitted curves to the experimental data [eq. (14)]. The measured scattering profiles of all systems bear a close resemblance to each other. SANS distributions for the present systems do not show any indication of peak. The value of $S(Q)$ was assumed unity because of negligible intermicellar interference. The SANS data were therefore fitted to following expression,

$$d\Sigma/d\Omega = n_m V^2{}_m (\rho_m - \rho_s)^2 < F^2(Q) > + B \tag{16}$$

where B is a constant that represents the incoherent scattering background. Scattered neutron intensity in a SANS experiment depends on the contrast factor $(\rho_m - \rho_s)^2$, i.e., the square of the difference between the average scattering length density of the particle and the average scattering length density of the solvent. The scattering length of hydrogen is negative ($=-0.3723 \times 10^{-23}$ cm) and that for deuterium is positive ($=0.6674 \times 10^{-12}$ cm). It is thus possible to have a very good contrast between the hydrogenous particle and the solvent by deuterating either the particle or the solvent. The contrast between the

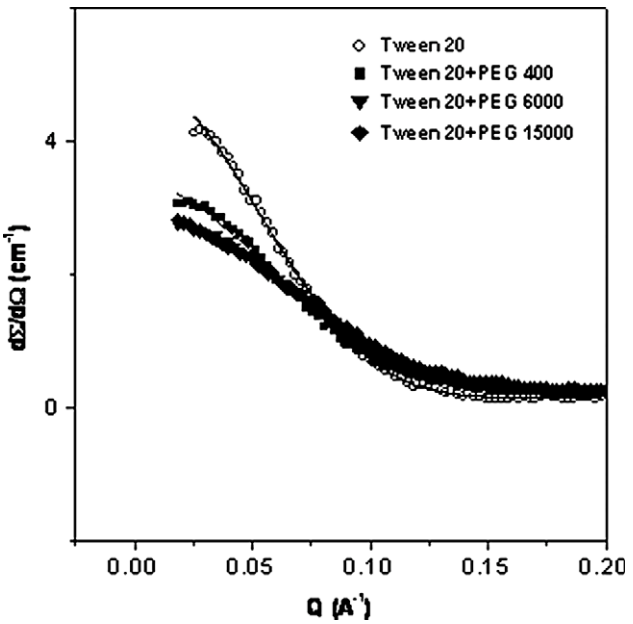

Figure 1 SANS distributions from micelles of Tween 20 (3 wt %) in D_2O in the presence of polyethylene glycols (10 wt %) at 30°C.

particle and the solvent can be varied by using mixed hydrogenated and deuterated solvent.

The different models for the shape of micelles, such as spherical, prolate and oblate ellipsoidal, and polydisperse sphere were used to calculate the scattering intensity. The parameters for the analysis were optimized by means of nonlinear least-square fitting program. It was found that oblate ellipsoidal model is the best-fitted model for the present Tween + glycol systems and extracted parameters look more consistent for this shape. The values of semi-

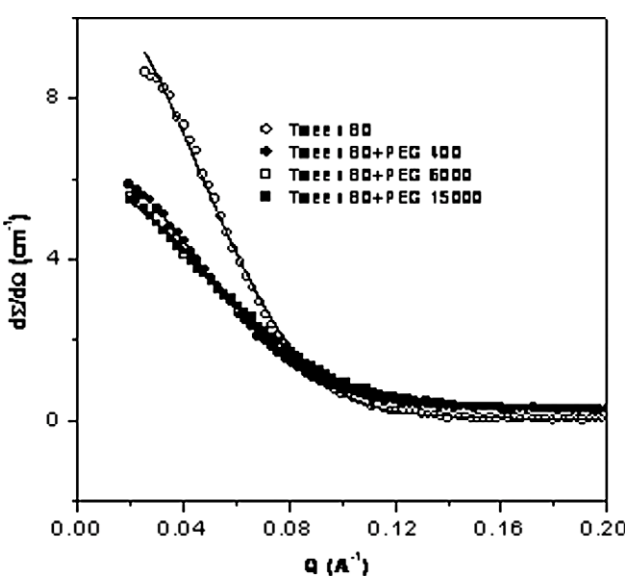

Figure 2 SANS distributions from micelles of Tween 80 (3 wt %) in D_2O in the presence of polyethylene glycols (10 wt %) at 30°C.

TABLE II
Values of Semimajor Axis (b), Semiminor Axis (a), Axial Ratio (b/a), Aggregation Number (N_{agg}), and Number Density (n_m) of Micelles of Tween (3 wt %) in the Presence of Polyethylene Glycols (PEGs) (10 wt %) of Different Molecular Weights

Additive	b (Å)	a (Å)	b/a	N_{agg}	n_m (cm^{-3})
Tween 20					
Blank	34.3	21.4	1.6	349	4.1×10^{16}
PEG 400	31.5	18.4	1.7	235	6.2×10^{16}
PEG 6000	29.5	10.9	2.7	123	11.7×10^{16}
PEG 15,000	29.8	8.3	3.6	96	15.1×10^{16}
Tween 80					
Blank	40.5	23.3	1.7	350	4.0×10^{16}
PEG 400	41.45	17.79	2.3	264	5.2×10^{16}
PEG 6000	39.27	14.31	2.7	190	7.3×10^{16}
PEG 15,000	38.18	14.16	2.7	178	7.8×10^{16}

minor axis (a) and semimajor axis (b) of the ellipsoidal micelles were calculated from the data analysis as explained earlier. The aggregation number of micelles, N_{agg} was calculated using the following expression,

$$N_{agg} = V_m/V_h \tag{17}$$

where V_m (=4/3 $\pi a^2 b$) is the micellar volume and V_h is the volume of hydrophobic part of the surfactant monomer. Using the calculated value of N_{agg}, number density of micelles, n_m, was calculated by using the following relation,

$$n_m/\text{cm}^{-3} = (C - CMC)N_A 10^{-3}/N_{agg} \tag{18}$$

where C is the concentration in mol dm^{-3} and N_A is the Avogadro's number. The parameters so obtained are listed in Table II. Polyethylene glycols PEG 400, 6000, and 15,000 are significantly increasing the values of axial ratio (b/a). It is clear that with the introduction of PEGs (10 wt %) into aqueous Tween (3 wt %) solution, the size of oblate ellipsoidal micelles is decreasing along the semiminor axis. The effect is most pronounced in case of PEG with highest molecular weight. The value of b/a is being maximum for PEG 15,000 amongst those used. Soni et al.[23] have also reported that in the presence of PEG 6000 (10% w/v), oblate ellipsoidal micelles of silicone surfactants based on poly(dimethylsiloxane)-graft polyethers grow along the semimajor axis. The addition of PEG (10 wt %) certainly reduces the values of N_{agg} of Tween 20 and Tween 80. The addition of PEG with more number of EG units reduces the N_{agg} of Tween 80 to more extent. It is due to the fact that PEG is facilitating the micelle formation due to which the aggregation number of micelles is decreasing. PEG would solubilize in the palisade layer of Tween micelles to produce mixed micelles.

TABLE III
Values of Semimajor Axis (b), Semiminor Axis (a), Axial Ratio (b/a), Aggregation Number (N_{agg}), and Number Density (n_m) of Micelles of Tween (3 wt %) in the Presence of TBPs (1 wt %) at 30°C

Additive	b (Å)	a (Å)	b/a	N_{agg}	n_m (cm^{-3})
Tween 20					
Blank	34.3	21.4	1.6	349	4.1×10^{16}
TBP_1	34.4	20.3	1.7	311	4.6×10^{16}
TBP_2	31.9	24.2	1.3	319	4.5×10^{16}
TBP_3	31.3	24.1	1.3	306	4.4×10^{16}
TBP_4	–	–	–	–	–
TBP_5	33.5	18.6	1.8	271	5.3×10^{16}
TBP_6	32.4	24.9	1.3	339	4.3×10^{16}
Tween 80					
Blank	40.5	23.3	1.7	350	4.0×10^{16}
TBP_1	38.2	20.3	1.9	256	5.4×10^{16}
TBP_2	36.0	23.7	1.5	265	5.2×10^{16}
TBP_3	35.2	24.9	1.4	267	5.2×10^{16}
TBP_4	–	–	–	–	–
TBP_5	39.1	20.4	1.9	270	5.1×10^{16}
TBP_6	38.1	27.0	1.4	339	4.1×10^{16}

SANS behavior of Tweens (3 wt %) in the presence of TBPs (1 wt %)

The SANS measurements have been made on 3 wt % aqueous solutions of Tween 20 and Tween 80 in the presence of various TBPs (1 wt %) of different composition (Table III). The SANS data for Tween 80 (3 wt %) in the presence of various TBPs (1 wt %) at 30°C do not show any indication of peak (Fig. 3). The value of $S(Q)$ was assumed unity because of negligible intermicellar interference. The SANS data were therefore fitted according to expression (16). It was found that oblate ellipsoidal model is the best-fitted model for the present systems and extracted parameters look more consistent for this shape. The parameters so obtained are listed in Table III. The size of micelles is decreasing in almost all cases. However, we do not get any regular trend of change in b/a value in this case. It is clear from Table III that the aggregation number of Tween (3 wt %) is decreasing in the presence of TBPs (1 wt %). TBP when present up to 1 wt % concentration does not effect the structural parameters of Tween micelles up to larger extent as it was observed in the presence of PEGs (10 wt %) of different molecular weights. The shape of micelles also remains same in the presence of TBPs (1 wt %). The experiments have also been done for Tween in the presence of TBPs (10 wt %) to study their effect on Tween micelles when compared with PEGs (10 wt %) and discussed in next section. Aswal and Kohlbrecher[24] have carried out contrast variation SANS experiments to study the effect of SDS on micellization of TBP $(EO)_{26}(PO)_{39}(EO)_{26}$ and reported that TBP form mixed micelles with SDS and the mixing of two components in the mixed micelles is uniform. They also observed that the shape of micelle was ellipsoidal and size of mixed micelles for fixed block copolymer concentration decreases with increase in the SDS concentration.

SANS behavior of Tween (3 wt %) in the presence of TBPs (10 wt %)

The SANS distribution for Tween (3 wt %) in the presence of various TBPs (10 wt %) at 30°C is shown in Figure 4 and various parameters obtained from

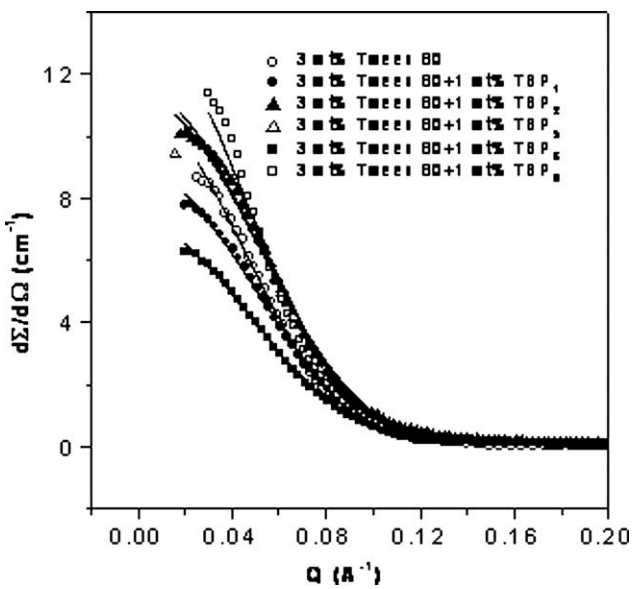

Figure 3 SANS distributions from micelles of 3 wt % Tween 80 in D_2O in the presence of TBPs (1 wt %) at 30°C.

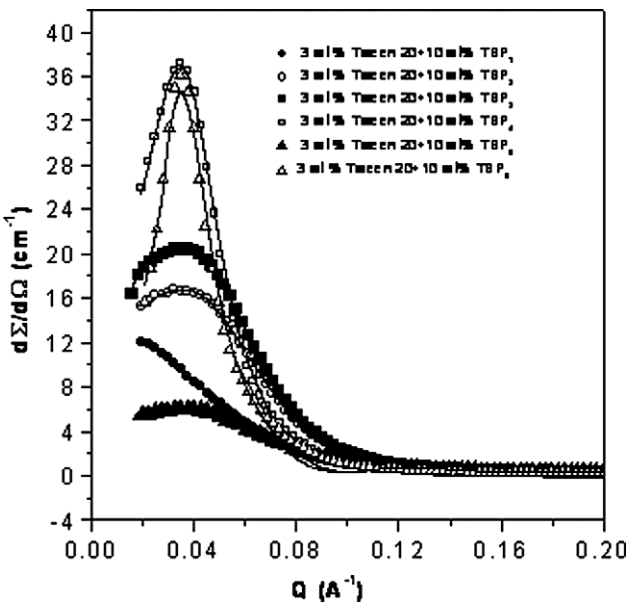

Figure 4 SANS distributions from micelles of Tween 20 (3 wt %) in D_2O in the presence of TBPs (10 wt %) at 30°C.

TABLE IV
Values of Core Radius (R_c), Hard Sphere Radius (R_{hs}), and Volume Fraction (ϕ) of Micelles of Tween (3 wt %) in Presence of TBPs (10 wt %) at 30°C

Additive	R_c (Å)	R_{hs} (Å)	ϕ
Tween 20			
TBP_1	35.5	119.2	0.05
TBP_2	33.2	54.7	0.07
TBP_3	34.5	55.9	0.07
TBP_4	44.9	72.5	0.1
TBP_5	29.8	57.9	0.06
TBP_6	43.2	90.1	0.2
Tween 80			
TBP_1	35.2	119.4	0.05
TBP_2	33.0	54.9	0.07
TBP_3	34.7	55.5	0.07
TBP_4	44.8	72.7	0.1
TBP_5	29.6	57.7	0.06
TBP_6	43.0	89.9	0.2

data analysis are listed in Table IV. It is quite obvious that different TBPs (10 wt %) are interacting differently with Tweens (3 wt %) micelles. The shape of micelles in all cases is found to be spherical. However the shape of micelle of Tweens (3 wt %) + TBPs (1 wt %) is oblate ellipsoidal (as discussed earlier). It means at high concentration the shape of mixed micelle is controlled by TBPs. Similar results have been obtained in case of Triton X-100 + TBP systems by Mahajan et al.[25] In all cases, R_c, R_{hs} are decreasing when compared with R_c, R_{hs} values observed for pure copolymers (5 wt %) as shown in Table V. Volume fraction of micelles in the solution is found to be almost same in all cases. The change in micellar size is related to the number of the copolymer molecules associated into micelle as well as to the solvation of micelle core and corona.

SANS behavior of pure TBPs (5 wt %)

The SANS distribution for TBPs (5 wt %) at 30°C is obtained and correlation peak in $d\Sigma/d\Omega$ is observed. Generally, this correlation peak in $d\Sigma/d\Omega$ arises due to interparticle structure factor $S(Q)$ and is seen at $Q_{max} \sim 2\pi/d$, where d is the average distance between two micelles. The interparticle distance

TABLE V
Values of Core Radius (R_c), Hard Sphere Radius (R_{hs}), and Volume Fraction (ϕ) of TBPs (5 wt %) at 30°C

TBP	R_c (Å)	R_{hs} (Å)	ϕ
TBP_1	–	–	–
TBP_2	47.2	129.0	0.1
TBP_3	51.9	143.1	0.09
TBP_4	52.4	96.0	0.08
TBP_5	–	–	–
TBP_6	57.1	115.1	0.25

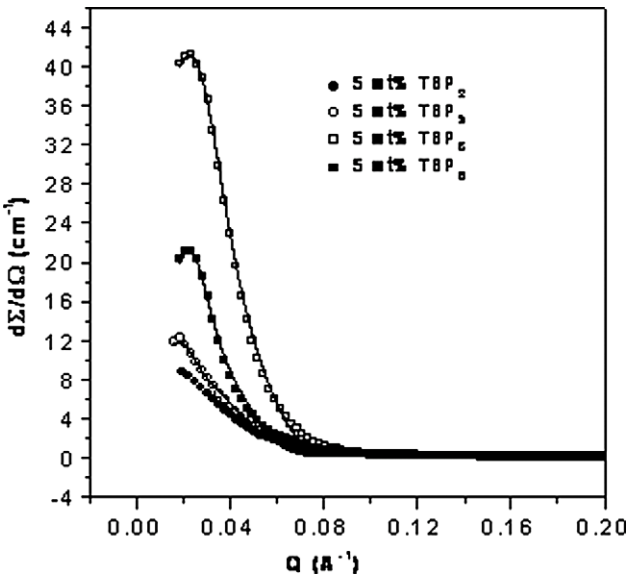

Figure 5 SANS distributions for TBPs (5 wt %) at 30°C.

decreases with increase in concentration and the peak shifts to higher Q value. When TBP solutions are prepared in D_2O, there is very good contrast between the hydrophobic core and the solvent, while there is a very poor contrast between the hydrated shell and the solvent. As a result $P(Q)$ depends only on the hydrophobic core radius as given in expression 13. The SANS distribution of various TBPs (5 wt %) at 30°C is shown in Figure 5. It was found that core-shell model is the best-fitted model for the present case. The micellar core, shell radii, and the hard sphere radii are illustrated in Figure 6. R_c and R_s are the radii of the micelle core and shell. R_{hs} is the hard sphere interaction radius. Figure 7 shows the SANS distributions from micelles of TBP_4 (5 wt %) and Tween 20 (3 wt %) in D_2O in the presence of TBP_4 (10 wt %) at 30°C. The various micellar parameters viz. R_c, R_{hs}, and ϕ obtained from SANS

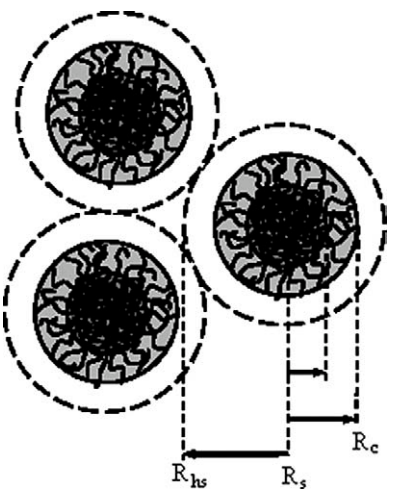

Figure 6 Schematic representation of spherical micelles.

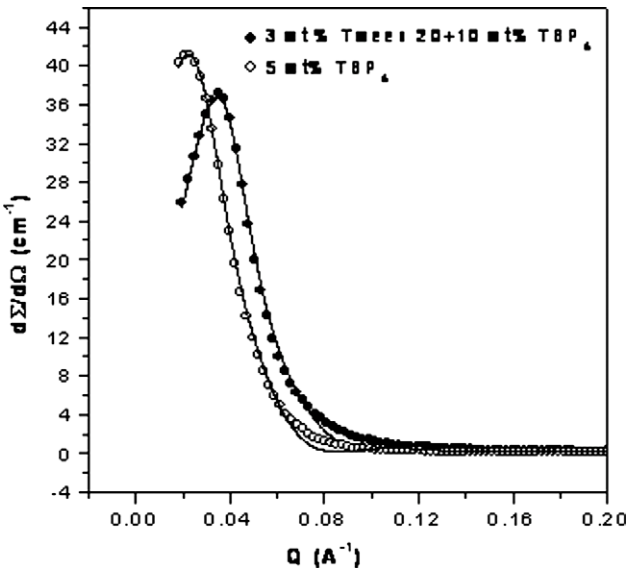

Figure 7 SANS distributions from micelles of TBP_4 (5 wt %) and Tween 20 (3 wt %) in D_2O in the presence of TBP_4 (10 wt %) at 30°C.

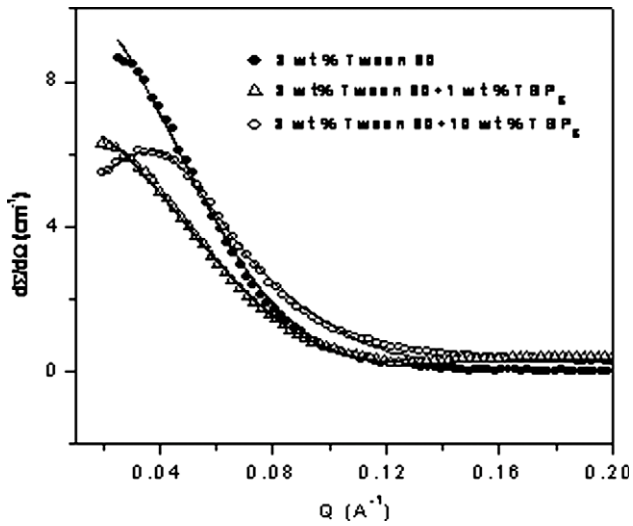

Figure 8 SANS distributions from micelles of Tween 80 (3 wt %) in D_2O in the presence of TBP_5 at 30°C.

analysis are given in Table V. Relatively higher values of R_c and R_{hs} observed for TBP_6 and are attributed to lager size of PEO and PPO block than other polymers. It has been already reported[26] that R_c, R_{hs}, ϕ, and N_{agg} are independent of any variation in copolymer concentration, as increase in concentration does not alter the characteristics of PEO or PPO block in its molecule. Hence, constancy in values of these parameters can be expected. The SANS results of Yang et al.[27] on 2.5 wt % Pluronic L64 in aqueous (D_2O) solution show that the micelles are well separated while intermicellar interaction remains strong and a core-shell model is more appropriate for the micelle morphology. In the analysis of SANS intensity distributions from P84[$(EO)_{19}(PO)_{43}(EO)_{19}$] and P104[$(EO)_{27}(PO)_{61}(EO)_{27}$] micelles in aqueous solutions, Chen et al.[28] nicely discussed a "cap and gown" model for the microstructure of micelles of L64, taking into consideration the polymer segmental distribution and water penetration profile in the core and corona regions, coupled with adhesive hard sphere model for describing the intermicellar interactions. The structure of micelles stays constant as a function of concentration. The micellar core is not completely dry but contains up to 20% volume fraction of solvent molecules at low temperatures. Contrasting the two polymers suggests that the micelles formed by a polymer with higher molecular weight tend to carry a larger volume fraction of solvent molecules.

The SANS distribution of Tween 80 (3 wt %) as a function of concentration of TBP_5 is shown in Figure 8. The data for Tween 80 (3 wt %) and Tween 80 (3 wt %) + TBP_5 (1 wt %) nearly coincide at high Q. At low Q value, there is pronounced concentration dependence. It is clear from Tables III–V that shape of Tween micelles is oblate ellipsoidal at low concentration of TBPs are present up to 1 wt % concentration. If polymer concentration is increased to 10 wt %, shape of micelles changes to spherical. Similar behavior was observed in case of other TBPs.

CONCLUSIONS

The addition of PEG (10 wt %) certainly reduced the values of N_{agg} of Tween. The addition of PEG additive with more number of ethylene glycol (EG) units reduced the N_{agg} of Tween to more extent. Shape of Tween (3 wt %) micelles is found to be oblate ellipsoidal at low concentration of TBPs (1 wt %) and changes to spherical at higher concentration of TBP (10 wt %). This indicates that at low concentration of TBP shape is controlled by surfactants (Tween 20 and Tween 80) while at high concentration of TBPs shape of mixed micelle is controlled mainly by TBPs.

References

1. Ogino, K.; Abe, M. Mixed Surfactant Systems; Marcel Dekker: New York, 1993.
2. Goddard, E. D.; Ananthapadmanabhan, K. P. Interactions of Surfactants with Polymers and Proteins; CRC Press: Boca Raton, FL, 1993.
3. Carrion, F. J.; Diaz, R. R. Tenside Surfact Deterg 1999, 36, 238.
4. Shiloach, A.; Blankschtein, D. Langmuir 1998, 14, 1618.
5. Couderc, S.; Li, Y.; Bloor, D. M.; Holzwarth, J. F.; Wyn-Jones, E. Langmuir 2001, 17, 4818.
6. Bakshi, M. S.; Bhandari, P.; Sachar, S.; Mahajan, R. K. Colloid Polym Sci 2006, 284, 1363.
7. Liao, C.; Choi, S.-M.; Mallamace, F.; Chen, S.-H. J Appl Cryst 2000, 33, 677.

8. Fairhurst, C. E.; Fuller, S.; Gray, J.; Holmes, M. C.; Tiddy, G. J. T. Handbook of Liquid Crystals; VCH: New York, 1998.
9. Nardin, C.; Hirt, T.; Leukel, J.; Meier, W. Langmuir 2000, 16, 1035.
10. Kelarakis, A.; Havredaki, V.; Yuan, X.; Yang, Y.; Booth, C. J. Mater Chem 2003, 13, 2779.
11. Mahajan, R. K.; Chawla, J.; Bakshi, M. S. Colloid Polym Sci 2004, 282, 1165.
12. Nagarajan, R.; Wang, C. C. Langmuir 2000, 16, 5242.
13. Ruiz, C. C.; Molina-Bolivar, J. A.; Aguiar, J. Langmuir 2001, 17, 6831.
14. Alexandridis, P.; Holzwarth, J. F. Curr Opin Colloid Interface Sci 2000, 5, 69.
15. Sastry, N. V.; Hoffmann, H. Colloids Surf A: Physicochem Eng Aspects 2004, 250, 247.
16. Bahadur, P. Curr Sci 2001, 80, 1002.
17. Aswal, V. K.; Goyal, P. S. Curr Sci 2000, 79, 947.
18. Skold, K.; Price, D. L. Methods of Experimental Physics-Neutron Scattering; Academic Press: London, 1986.
19. Hayter, J. B.; Penfold, J. Colloid Polym Sci 1983, 261, 1022.
20. Chen, S. H.; Lin, T. L. Methods of Experimental Physics-Neutron Scattering; Academic Press: New York, 1987.
21. Guinier, A.; Fournet, J. Small Angle Scattering of X-Rays; Wiley InterScience: New York, 1955.
22. Glatter, O.; Kratky, O. Small Angle X-Ray Scattering; Academic Press: London, 1982.
23. Soni, S. S.; Sastry, N. V.; Joshi, J. V.; Seth, E.; Goyal, P. S. Langmuir 2003, 19, 6668.
24. Aswal, V. K.; Kohlbrecher, J. Pranama J Phys 2004, 63, 339.
25. Mahajan, R. K.; Vohra, K. K.; Aswal, V. K. Colloids Surf A: Physicochem Eng Aspects 2008, 326, 48.
26. Jain, N. J.; Aswal, V. K.; Goyal, P. S.; Bahadur, P. Colloids Surf A: Physicochem Eng Aspects 2000, 173, 85.
27. Yang, L.; Alexandridis, P.; Staytler, D. C.; Kositza, M. J.; Holzwarth, J. F. Langmuir 2000, 16, 8555.
28. Chen, S. H.; Liao, C.; Fratini, E.; Baglioni, P.; Mallamace, F. Colloids Surf A: Physicochem Eng Aspects 2001, 95, 183.